

The high-speed two-channel analyzer of optically dense aerosol emissions based on diode optocouplers with a wavelength of 0.65 and 3.4 microns

© A.V. Zagnit'ko, V.V. Pimenov, S.E. Sal'nikov, D.Y. Fedin, V.I. Alekseev, I.D. Matsukov, S.M. Velmakin, N.P. Zaretsky, E.V. Chernenko

National Research Center „Kurchatov Institute“,
123182 Moscow, Russia
e-mail: azagnitko@yandex.ru

Received October 21, 2022

Revised December 22, 2022

Accepted December 22, 2022

A two-channel analyzer of optically dense flammable aerosol fluxes based on two parallel diode optocouplers with a wavelength of electromagnetic radiation $\lambda = 0.65$ and $3.4\ \mu\text{m}$, a speed of $\tau \leq 0.05$ s and the transmission of digitized data to a server up to 1200 m away via the RS-485 interface has been developed. Its design and characteristics in the process of detecting particle streams with a diameter of 0.2 to $5000\ \mu\text{m}$ with an optical density of $D \leq 3.5$ are described. It is shown that the values of the ratio of wave attenuation coefficients with $\lambda = 0.65$ and $3.4\ \mu\text{m}$ to the droplet size calculated on the basis of the theory of radiation scattering M_i are consistent with the experimental ones. The created aerosol analyzer can be used in the express analysis of technogenic airborne emissions of fuel liquids and for the development of large-scale generators of explosive type when creating pulse barriers from clouds of finely dispersed aerosol in the atmosphere.

Keywords: aerosol analyzer, speed, diode optocouplers, infrared and visible radiation, attenuation factor, optically dense emissions, M_i scattering theory, fuel liquids.

DOI: 10.21883/TP.2023.02.55472.236-22

Introduction

Express analysis of optically dense aerosol emissions into the atmosphere and the development of explosive-type generators for the rapid creation of large-scale barriers of fine droplets on the path of the spread of toxic and combustible clouds is of interest for industrial safety systems of objects, production and storage of fuel liquids (kerosene, gasoline, fuel oil, diesel fuel (DF), oil, heptyl, alcohol, etc.). During technogenic fuel emissions in the form of jets and spills on the ground there is a high probability of the formation of explosive and flammable fuel-air mixtures (FAM) with a volume of more than $10^4\ \text{m}^3$ [1–5].

The regularities of FAMs formation and their further transformation are characterized by a large number of variable parameters, which are determined both by the properties of the gas-droplet phase and the environment and have a number of features, such as high speed of liquid ejection, short formation time of large-scale clouds, non-stationarity of polydisperse aerosol evolution processes under aerodynamic split conditions, cavitation and evaporation of droplets, turbulent coagulation and sedimentation [5–8].

The analysis of FAM emissions is quite complicated, since it is necessary to measure the fluctuating characteristics of particles with data transfer to a remote server, and devices for their scanning must have a response $\tau \leq 0.1$ s, operate

at gas-droplet flow rates up to hundreds of meters per second, and be resistant to impulse action of excessive gas pressure ($> 10^5$ Pa) [1–10].

It is known that single-channel and two-channel laser analyzers of aerosol flows (optocouplers) with an inertial droplet separator with a diameter of $d > 15\text{--}20\ \mu\text{m}$ and a radiation wavelength of $\lambda = 0.6\text{--}0.7\ \mu\text{m}$ were designed [3,4]. These devices make it possible to measure with $\tau \leq 0.05$ s the dynamic values of the optical density $D = \lg(I_0/I) \leq 3.5$ and the specific surface concentration of droplets $S = \pi \langle d^2 \rangle N$ (m^2/m^3), as well as the value of their root-mean-square deviation at a volume concentration of droplets less than 0.1% vol. Here I_0 and I — radiation intensities without and in the presence of FAMs, respectively, in the optical channel of the optocoupler; $\langle d^2 \rangle^{0.5}$ — root-mean-square diameter of droplet with differential size distribution $f(d)$; count concentration N [1–5]. In the case of common log-normal distribution of droplets by diameters, the value $\langle d^2 \rangle = \langle d \rangle^2 \exp(\ln^2 \sigma)$, where $\langle d \rangle$ — arithmetic mean droplet diameter and σ — standard geometrical deviation [5]. For an arbitrary particle size distribution $\langle d^2 \rangle = \langle d \rangle^2 (1 + q^2)$, where q — variation parameter. The digitized data is transferred to the server with an interval of 0.001–0.01 s.

According to the Mie theory [5–8] the change in the energy flow of electromagnetic waves is caused by their

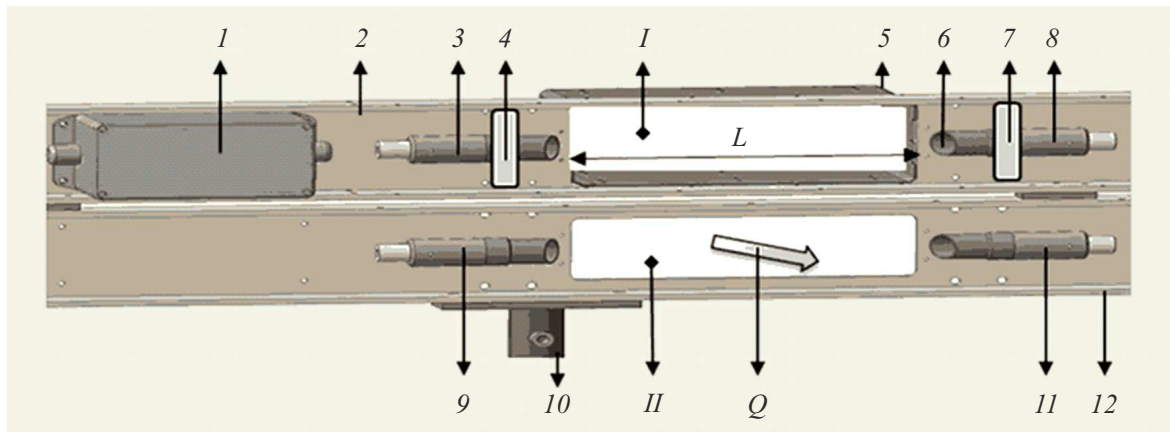


Figure 1. Schematic diagram of two-channel laser aerosol analyzer (explanations in the text).

scattering and absorption by uncharged droplets. Its weakening in accordance with Bouguer’s law can be calculated as

$$\lg(I_0/I) = KL, \tag{1}$$

where K — volume attenuation coefficient and L — thickness of the scattering layer [5–8]. Formula (1) is valid for single scattering of radiation by droplets and for a sufficiently large number of scatters $NS_1L \gg 1$ with a distance between them of more than $(4–5)d$, where S_1 — cross-section area of the laser beam in the particle analysis zone [7]. Let us point out that these conditions were fulfilled in the studies carried out (see Sections 1 and 2).

In the case of a monodisperse particles flow $K = N\beta(m)\pi d^2/4$, where $\beta(m)$ is the attenuation coefficient of radiation by droplet from the value of the Mie scattering parameter $m = \pi d/\lambda$ [5–8]. A generalization for polydisperse droplets in the approximation that the contribution from each of the droplet groups to K is additive has the form [3–5,7]:

$$K = N\left(\frac{\pi}{4}\right) \int_d^{\square} d^2 f(d)\beta(m)dd. \tag{2}$$

The use of Bouguer’s law assumes that all the energy scattered by the droplets is removed from the radiation beam, and the coefficient K is determined by integrating the energy scattered in different directions, including the forward direction. For $m > 10$ $K = F(Z, d/\lambda) \times (S/4)$, where $Z = md_1/2L$, d_1 — the diameter of the receiving lens and $F(Z, d/\lambda)$ — a corrective function that takes into account the indicatrix of radiation scattering by droplets and the size of the optical zone of the optocoupler [7]. $F(Z, d/\lambda)$ tend to the limit $\alpha = 1, 1.5$ and 2 at $Z \gg 1, \rightarrow 1$ and $\rightarrow 0$ respectively [7]. In this case, D and K can be calculated

using the formulas [5–7]:

$$D = \alpha\pi N\left(\frac{L}{9.2}\right) \int_d^{\square} d^2 f(d)dd$$

$$= \alpha\pi N\langle d^2 \rangle \left(\frac{L}{9.2}\right) = \alpha SL/9.2; \tag{3}$$

$$K = \alpha S/4. \tag{4}$$

The patented laser analyzers of FAMs do not allow the express analysis of fluctuating sizes of fine droplets in optically dense aerosol emissions [3,4]. The aim of the paper was to develop a high-speed with $\tau \leq 0.05$ s two-channel aerosol flow analyzer based on two parallel diode optocouplers with $\lambda = 0.65 \pm 0.005 \mu\text{m}$ and $\lambda = 3.4 \pm 0.2 \mu\text{m}$ for express analysis of fluctuating values D, S and d with data transfer to remote server up to 1200 m via RS-485 interface. According to the Mie theory the ratio β of the attenuation coefficients of radiation with wavelengths $\lambda = 0.65$ and $3.4 \mu\text{m}$ from $d = 0.4–1000 \mu\text{m}$ [5–8], and they were compared with experimental values β for particles with diameter greater than $0.2 \mu\text{m}$ and mass concentration $M \approx 0.001–4.0 \text{ kg/m}^3$. The choice of such a wide range of particle parameters change was due to the fact that in large-scale emissions of liquids into the atmosphere their rapid variation is observed in a wide range of values $d \approx 0.5–10^4 \mu\text{m}$ and $M \approx 0.001–5.0 \text{ kg/m}^3$ [3–5].

1. Experimental part

Fig. 1 shows a schematic diagram of high-speed two-channel aerosol emission analyzer based on two diode optocouplers. The first optocoupler with a wavelength of $\lambda = 3.4 \pm 0.2 \mu\text{m}$ in channel I contains an immersion LED 3 (LED34TO8TEC) and a photodiode 8 (PD34TO8TEC) [9,10] connected by a flexible mechanical connection with the housing 2, adjusting elements 4 and 7 to adjust the diode optocoupler to the maximum value

of the output signal of the photodiode. As a result, the misalignment of the optical scheme and radiation patterns of the LED 3 and the sensitivity of the photodiode 8 is eliminated. The second diode optocoupler in channel II with a wide radiation pattern and $\lambda = 0.65 \pm 0.005 \mu\text{m}$ is made with rigid fixation of the semiconductor laser 9 (ADL-65055TA2) and photodiode 11 (BPW24R) inside the housing 12. Parallel metal housings 2 and 12 are made with rectangular windows for a convective gas-droplet flow Q through channels I and II. The external electronic unit 1 is fixed in the housing 2 and is designed for power supply, control, temperature stabilization and synchronous transmission of digitized signals from two optocouplers every 0.02 s via twisted pair using the RS-485 interface to remote up to 1200 m secure server for their further processing and analysis. The choice of optocoupler wavelengths was determined by the insignificant absorption of radiation by atmospheric water vapor.

Both immersion semiconductor devices 3 and 8 are equipped with a system for temperature stabilization of the emitter 3 and photodetector 8 (using Peltier elements) at the level set during their adjustment (from 285 to 300 K) [3,9,10]. The temperature values are continuously read by the microprocessor for monitoring and, together with the values of the working and background signals of the photodiodes 8 and 11, are transmitted via the RS-485 interface to remote server (not shown in Fig. 1).

The characteristics of two-channel optocoupler were studied at the test bench for the analysis of particles and gas-vapor mixtures of hydrocarbons [3–4,11]. Aerosol flows of moderately polydisperse droplets of water, glycerin, kerosene, diesel fuel, white spirit, marine fuel oil F5 and turbine oil TP22 with droplet diameter of less than $15 \mu\text{m}$ and $\sigma \leq 1.7$ were obtained using a fog generator „TO-52“ (RF) at a temperature of 293–380 K and a cold ultrasonic fogger with 12 piezoceramic membranes „MHB12-UH“ (China). When obtaining larger droplets with $d = 20–5000 \mu\text{m}$ and $\sigma \approx 2–3$, electric pneumatic atomizers of liquids of the type „EKRP-600/0.8, Kalibr“ (RF), „Karcher K3“ and „W590 Flexio, Wagner“ (Germany) were used. When generating a mixture of submicron solid and liquid particles, free combustion, distillation, and pyrosynthesis of cigarette tobacco compounds in the air stream were carried out. Besides, local pulsed ejections of liquids in the form of submerged jets with a speed of up to 50 m/s and a length of 5–10 m were studied at Reynolds numbers $\text{Re} = U_1 d \rho / \eta < 10^4$ with their aerodynamic fragmentation at Weber numbers $\text{We} = \rho(U_1 - U)^2 d / \delta < 10^5$ [3–5]. Here ρ , η and U — density, dynamic viscosity and air speed, respectively, δ — liquid surface tension coefficient, d — diameter of droplets and liquid fragments, U_1 — their speed. Droplets and liquid fragments were created using a pulsed aerosol generator with a source of air compressed to 8 MPa with a volume of 0.2 m^3 under normal conditions. The gas-droplet flow was formed during a bubble flow of compressed air through a layer of atomized liquid at

an initial speed of about 250 m/s during the air pressure reduction by solenoid valve for maximum 0.3 s.

Analysis of large-scale FAMS up to 10^7 m^3 was carried out in the process of pulsed sputtering of fuels during the initiation of high-energy materials (HEM). In these experiments the Reynolds numbers in the flow did not exceed 10^6 , and the aerodynamic fragmentation of droplets occurred at Weber numbers below 10^5 [3–5].

The size and concentration of the particles were determined by the ultramicroscopic method in a cuvette, using a six-stage impactor with round nozzles and a microscope, by the gravimetric method, and also by sampling particles on analytical glass fiber filters. The images with droplet imprints in order to estimate their size distribution were processed using the ImageJ software package, taking into account the measured coefficient of droplet spreading on the filter material [11,12]. Besides, to estimate the size and concentration of particles, their unipolar charging with corona discharge gas ions was used, followed by measurement of the transfer current of charged particles during their deposition on the fibers of the electrically conductive filter connected to the electrometric amplifier [3–5,11]. Infrared photometry of fuel droplets deposition on filters was carried out with a concentration meter „KN-2m“ (RF). Hydrocarbon gas mixtures were analyzed by infrared analyzers with an immersion optocoupler and Mipex sensors [3]. The surface concentration of droplets in the ejection and its speed were measured by laser optocouplers [5].

Fig. 1 shows: 1 — electronic unit; 2 and 12 — metal housings with rectangular windows for aerosol flow Q through channels I and II of optical analysis of aerosols with scattering layer length $L \approx 0.07–0.1 \text{ m}$; 3 and 8 — semiconductor immersion LED and photodiode ($\lambda = 3.4 \text{ micron}$), respectively, with their adjusting elements 4 and 7; 5 — inlet thin-wall rectangular channel connected with rectangular holes for flow Q through channels I and II; 6 — photodiode lens with diameter d_1 (ratio $d_1/L \approx 0.06–0.08$); 9 and 11 — semiconductor LED and photodiode ($\lambda = 0.65 \text{ micron}$), respectively; 10 — mount for the analyzer securing on a mast or cable.

2. Results and discussion thereof

The optocoupler response τ was determined by measuring the voltage at the output of the signal amplifier of photodiodes 8 and 11 as a function of time at more than 300 exchanges of aerosol volume per second by filtered air in channels I and II. It is shown that $\tau \leq 0.05 \text{ s}$ at the electronic unit response $\tau_0 \approx 25 \mu\text{s}$ with data transfer to the remote server every 0.02 s. The method of τ_0 analysis is described in [3].

In the process of ejection of various liquids with speeds up to 50 m/s, bipolar electrification of droplets with practically zero space charge was observed. The droplets' charges were significantly less than the charges during their classical impact and diffusion charging by unipolar corona

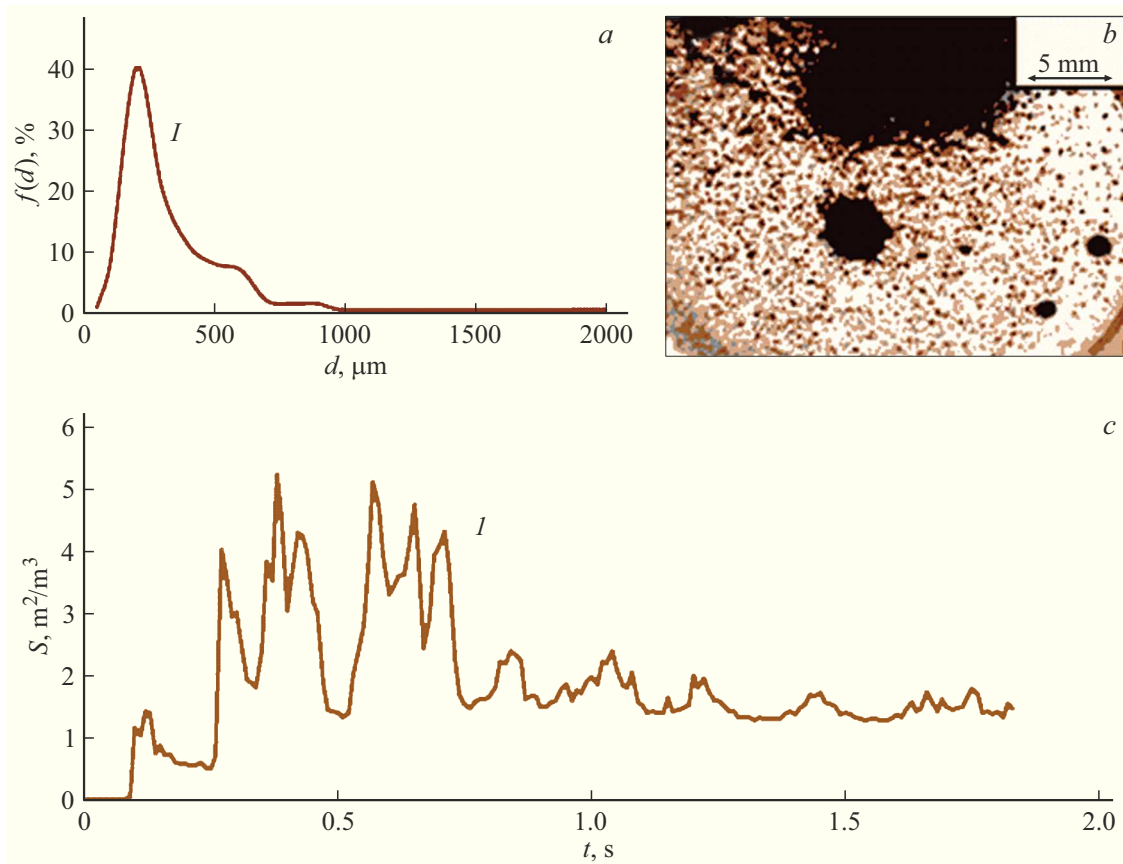


Figure 2. Characteristics of aerosol during pulsed release of fuel oil F5 into the atmosphere at a height of 8 m ($T = 311$ K): *a* — droplet size distribution $f(d)$ (curve *I*), *b* — photograph of their black-brown imprints on the filter surface; *c* — specific surface concentration S of droplets vs. time t (curve *I*).

discharge ions [5,11]. In this case, the electrical resistivity R and permittivity ε of liquids varied over a wide range. So, if in the case of fuels (kerosene TS-1, white spirit, diesel fuel, fuel oil F5, oil TP22) the measured values $R > 10^{10} \Omega \cdot \text{m}$ and $\varepsilon \approx 2$, then for water and glycerin: $R = 30$ and $610 \Omega \cdot \text{m}$ and $\varepsilon = 80$ and 43 , respectively. As a result, the bipolar electrification of droplets was not taken into account in the analysis of radiation scattering.

It is shown that, with accuracy sufficient for practice, the size distribution of particles, in which there are much more small droplets than large ones, can be approximated by a logarithmically normal function. As an example, Fig. 2, *a* shows the experimentally obtained and close to log-normal distribution $f(d)$ (curve *I*) of F5 fuel oil droplets sampled on a glass fiber filter. Droplets were aspirated at a height of 8 m. Processing of the obtained images (black-brown droplets on the white surface of the filter, see photograph *I* in Fig. 2, *a*) and their analysis were carried out using the ImageJ software package [12], resulting in d varying from 20 to 2000 μm , $\langle d \rangle = 348 \mu\text{m}$ and $\sigma = 2.4$. Practically no droplets below 20 μm in diameter were detected. This agrees with the calculations, according to which, at an initial gas-droplet ejection speed of about 100 m/s the aerodynamic fragmentation of droplets with

$d < 20 \mu\text{m}$ does not occur, since the Weber number for such droplets is below the critical value ($We < 10$). The characteristic time of gas-droplet ejection of fuel oil with a volume of up to 10^5m^3 was less than 2 seconds, which was recorded by measuring the specific surface of droplets from time to time (see Fig. 2, *b*). The value S was calculated by the formula (3) with $\alpha = 1$, since the Mie parameter is $m > 10^3$ and $Z > 50$.

Note that similar results were obtained during explosive spraying of diesel fuel and oil from the Astrakhan field with a viscosity of $\approx 5\text{--}7 \text{Pa} \cdot \text{s}$ at 320 K with FAM volume of about 10^5m^3 .

Fig. 3 shows the experimental dependences of the optical density D on time for water mist droplets ($\langle d \rangle = 4 \mu\text{m}$ and $\sigma = 1.6$) (Fig. 3, *a*) and oil mist with $\langle d \rangle = 0.6 \mu\text{m}$ and $\sigma = 1.6$ (Fig. 3, *b*). Gas-droplet flows were obtained using an ultrasonic fogger „MHB12-UH“ and generator „TO-52“ respectively. Curves *1* and *2* — graphs of time-synchronized fog optical densities in channels I and II at $\lambda = 3.4$ and $0.65 \mu\text{m}$. In this case, a significant dependence D of finely dispersed droplets on d and λ was recorded, which agrees with the calculations according to the Mie theory. The radiation absorption by water vapor was practically not observed in both channels.

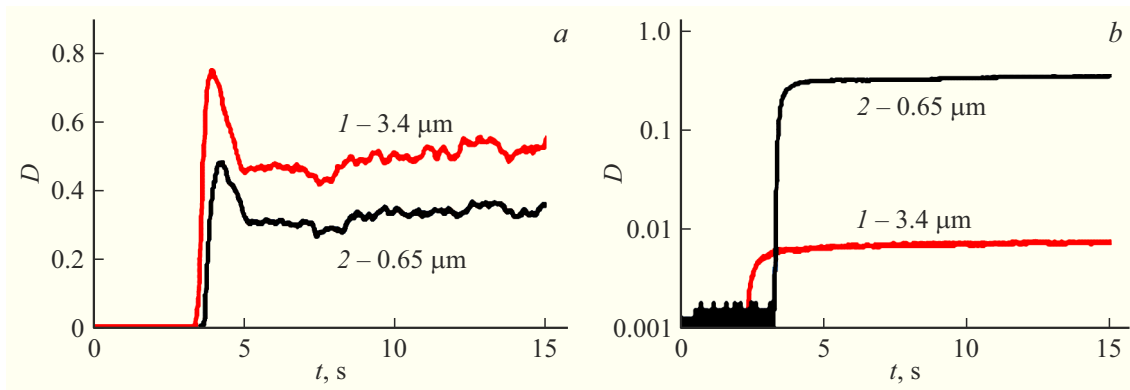


Figure 3. Graphs of optical density D vs. time t for a stationary droplet flow.

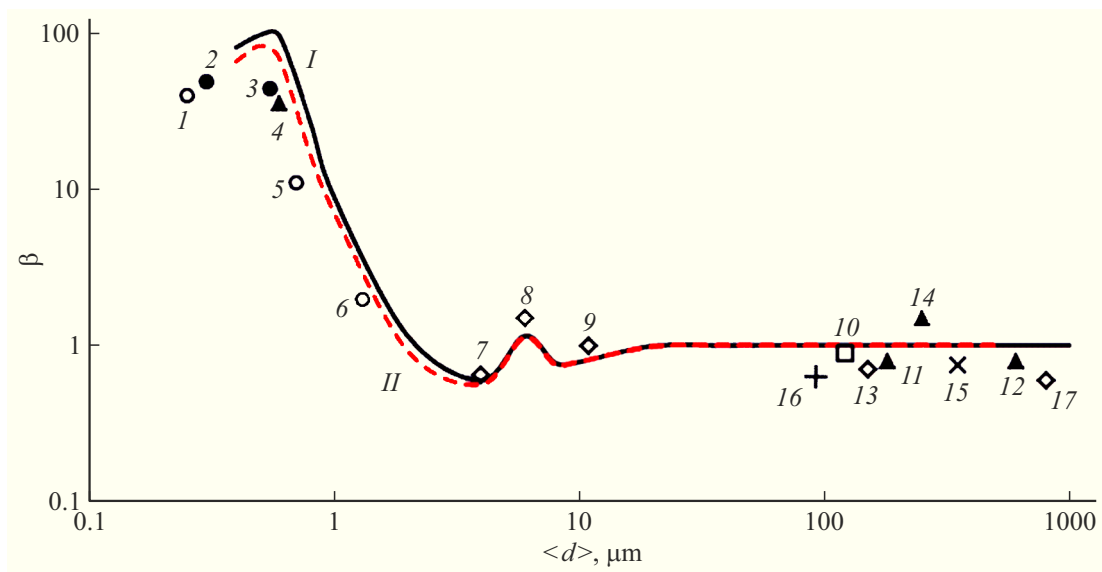


Figure 4. Graphs of the calculated value β (curves I and II) vs. arithmetic mean diameter $\langle d \rangle$ of droplets and experimentally obtained points ($I-17$). The reference information of these values of points of coefficients of radiation attenuation by droplets β in Fig. 4 are summarized in Table.

Fig. 4 shows the dependences of the ratio of the coefficients of radiation attenuation by droplets $\beta = N\beta_{II}(m)/N\beta_I(m)$ on the droplet size d : curve I — calculation according to Mie theory, dots ($I-17$) — experimental values, $\beta_I(m)$ and $\beta_{II}(m)$ — coefficients of radiation attenuation by droplets of diameter d at $\lambda = 3.4$ and $0.65 \mu\text{m}$, respectively. Their values are given in [5–8]. The experimental values β are determined by the ratio of the volumetric coefficients of radiation absorption in channels I and II — $\beta = K_{II}/K_I$, measured simultaneously. The dots $I-17$ correspond to the Table data. Curve II is calculated according to Mie theory for wavelengths $\lambda = 3.4$ and $0.4 \mu\text{m}$. Its comparison with the I curve shows that the reduction in channel II of the radiation wavelength from $0.65 \mu\text{m}$ to $0.4 \mu\text{m}$ at a constant infrared radiation wavelength ($3.4 \mu\text{m}$) does not improve the accuracy of express analysis of droplet size. As can be seen from the Figure, for droplet sizes $d > 5-10 \mu\text{m}$

the ratio of attenuation coefficients in channels I and II can be considered independent of the droplet size and wavelength with accuracy sufficient for practice. Coloring water, kerosene and glycerin with methylene blue did not affect the experimental values β in experiments, which is consistent with the theory [5]. Thus, a satisfactory agreement between the experimental data and the calculated ones was obtained. Their slight discrepancy for polydisperse aerosols is due to the fact that full consideration of the optical zone size of the optocoupler and the correction function $F(Z, d/\lambda)$ in the analysis β for aerosols with $\sigma > 1.7$ was not carried out due to the complexity of calculating the influence of a wide range of droplet sizes on $F(Z, d/\lambda)$.

It follows from the analysis of the obtained results that the detection of $\beta \approx 1$ values with $\tau \leq 0.05$ s when analyzing the evolution of fuel liquid emissions allows us to conclude that the main range of droplet sizes exceeds $5 \mu\text{m}$, and their fine fraction is practically absent. This result was recorded

Values M , σ , $\langle d \rangle$ and $\langle d^2 \rangle^{0.5}$ for droplets of fuel liquids, water, glycerin, TP22 oil, mixture of solid and liquid cigarette smoke particles with error $\pm 10\%$

Substance (GOST)	N [*]	M , kg/m ³	σ	$\langle d \rangle$, micron	$\langle d^2 \rangle^{0.5}$, micron
Oil TP22 (32-74)	1	0.0025	1.6	0.25	0.28
	5	0.001	1.6	0.7	0.78
	6	0.002	1.7	1.3	1.5
Tobacco (3935-2000)	2	0.04	2.5	0.3	0.46
	3	0.06	2.5	0.55	0.84
Kerosene TS-1 (10227-86)	4	0.01	1.6	0.6	0.67
	11	0.16	2.5	160	244
	12	0.5	2.5	600	913
	14	0.35	2.2	250	341
Water (P51232-98)	7	0.045	1.6	4	4.47
	8	0.055	1.6	6	6.7
	9	0.05	1.6	11	12.3
	13	0.35	2.2	150	205
	17	4	3	800	1468
Fuel oil F5 (10585-99)	15	0.25	2.4	348	510
Glycerin (6259-75)	16	0.33	2.3	95	134

Note. N^{*} in the Table corresponds to the dot number in Fig. 4.

for pulsed with HEM use ejection of fuels and inefficient aerodynamic fragmentation of droplets with $d < 5 \mu\text{m}$ at Weber numbers $We < 5$.

Finding β in the range of values from 2 to 100 means that in the analyzed FAM the main concentration is fluctuating in size finely dispersed droplets with a diameter of less than $3 \mu\text{m}$. In this case, their average size is determined by β .

Note that in the study of FAM the radiation absorption by vapors of atmospheric water and hydrocarbons was estimated, since, according to the additive law $D = D_A + D_P$, where $D_A = \lg(I_o/I_A)$ and $D_P = \lg(I_o/I_P)$ — optical density of aerosol and vapor-gas components, and I_A and I_{II} — their radiation intensities after FAM, respectively [5–8].

It is shown that almost no radiation attenuation was observed when passing through channels I and II a vapor-air flow filtered from droplets with a humidity of more than 95% at $T = 293\text{--}300\text{ K}$. Their density was $D_P < 0.01$ and did not exceed the background level. Similarly, in channel II at $\lambda = 0.65 \pm 0.005 \mu\text{m}$, the attenuation of wave intensity by hydrocarbon vapors was also not fixed. The same result was obtained in the detection of methane and regasified liquefied gas (LNG) with a volume concentration of $C = 1\text{--}99\%$ vol. These results are consistent with the data of analysis of the spectra of radiation absorption by water vapor and hydrocarbons.

Analysis of FAM vapors in channel I with $\lambda = 3.4 \pm 0.2 \mu\text{m}$ at $L = 0.1\text{ m}$ showed that their value is $D_P < (0.05\text{--}0.1)D_A$. Note that in large-scale fuel ejections

with the formation of submerged jets and clouds with a volume of 10^4 to 10^7 m^3 the pairs, as a rule, were unsaturated. Apparently, this is due to their intense dilution with air and the relatively slow rate of droplets evaporation during their decomposition.

Note that the evaporation rate and the efficiency of aerodynamic crushing of droplets of light alkanes and LNG, as well as the pressure of their saturated vapors are significantly higher compared to similar parameters of the studied droplets of kerosene, fuel oil, diesel fuel, glycerin, Astrakhan oil, ethyl alcohol, white spirit and heptyl. For example, at $T = 293\text{ K}$, according to the model of convective energy exchange between a cryogenic droplet and the surrounding vapor-gas medium, the evaporation time of 50% of the volume of boiling methane droplets is proportional to the square of their diameter, and at $d = 1$ and $10 \mu\text{m}$ is respectively $4 \cdot 10^{-6}$ and $4 \cdot 10^{-4}\text{ s}$ both in air and in a cloud of vaporous methane with a pressure of 10^5 Pa [3,4]. Note that using the classical diffusion evaporation theory of Maxwell-Langmuir as well as Knudsen and Hertz for the boiling drops immobile in relation to the vapor-gas medium is not correct, as their temperatures are substantially different [5].

As a result, it is not possible to analyze the size of such rapidly evaporating fine droplets of light alkanes by β . This effect was observed when creating gas-droplet flows of methane and LNG. However, channel I was used to detect the kinetics of formation of flammable concentrations of methane, ethane, propane, butane, and regasified LNG. Their optical density significantly depended on the type and magnitude of the explosive concentration of alkanes and varied in the range $D_P \approx 0.02\text{--}0.4$ at $L = 0.1\text{ m}$ [3,4]. We indicate that the values of their lower and upper concentration flammability limits are C (% vol.) $\approx (4.4/17.0, \text{ methane})$; $(2.5/15.5, \text{ ethane})$; $(1.7/10.9, \text{ propane})$ and $(1.4/9.3, \text{ butane})$ [1,2].

Conclusion

A two-channel analyzer of optically dense aerosol flows and clouds based on diode optocouplers with $\lambda = 0.65$ and $3.4 \mu\text{m}$ was developed and patented for measuring of fluctuating in a wide range optical density, concentration and size of dispersed particles with a speed up to 0.05 s . Experimental and calculated, according to the Mie theory, values of the ratio of the attenuation coefficients of infrared and visible waves by droplets, depending on their size, are consistent.

A high-speed optocoupler can be used to analyze optically dense gas-drop flows of fuel assemblies during their pulsed outflow into the atmosphere, as well as in the development of explosive-type aerosol generators for obtaining finely dispersed droplets with a developed surface in order to instantly create liquid-droplet barriers at propagation paths of emissions of fuels, flame, toxic or radioactive gases.

The possibility of integrating the created high-speed network of two-channel laser analyzers of aerosol emissions with the industrial safety monitoring systems of fuel and energy complex facilities, as well as their use both for analyzing the evolution of emergency emissions and for engineering calculations of submerged gas-droplet jets is shown.

The technical characteristics of the created two-channel analyzer of technogenic emissions of fuel liquids with the formation of large-scale FAMs exceed the parameters of domestic and foreign analogues.

Funding

The study was performed on the subject „Development of physical and technical methods of measurement of parameters of aerosol and vapor-gas clouds occurring in large-scale emergencies on F&E facilities and creation of experimental samples of the systems of diagnostics of aerosol clouds“ as per the order № 2748 dated October 28, 2021.

Conflict of interest

The authors declare that they have no conflict of interest.

References

- [1] C.J.R. Coronado, J.A. Carvalho, J.C. Andrade, E.V. Cortez, E.S. Carvalho, J.C. Santos, A.Z. Mendiburu. *J. Hazardous Materials*, **241–242**, 32 (2012). DOI: org/10.1016/j.hazmat.2012.09.035.
- [2] *Dannye for goryuchim gazam i param, odnosyaschiesya k ekspluatatsii elektrooborudovaniya*. (GOST R 51330.19-99 (IEC 60079-20-96)) (in Russian)
- [3] A.V. Zagnit'ko, I.D. Matsukov, V.V. Pimenov, S.E. Salnikov, D.Yu. Fedin, V.I. Alekseev, S.M. Vel'makin. *ZhTF*, **92**(6), 783 (2022) (in Russian). DOI: 10.21883/JTF.2022.06.52505.325-21
- [4] A.V. Zagnit'ko, N.P. Zaretskiy, I.D. Matsukov, V.I. Alekseev, S.M. Vel'makin, D.Yu. Fedin, V.V. Pimenov, S.E. Sal'nikov. *Gazovaya promyshlennost'*, **5**, 82 (2021). (in Russian)
- [5] P. Rajst. *Aerozoli. Vvedeniye v teoriyu* (Mir, M., 1987), 280 s. (in Russian)
- [6] Van de Hulst G. *Rassivanie sveta malymi chastitsami* (IIL, M., 1961), 536 s. (in Russian)
- [7] V.E. Zuev, M.V. Kabanov. *Optika atmosfernogo aerosolya* (Gidrometeoizdat, L., 1987), 255 s. (in Russian)
- [8] G.P. Grudinskaya. *Rasprostranenie radiovoln* (Vasshg. sh., 1975), 280 s. (in Russian)
- [9] ООО „IoffeLed“. www.ioffeled.com. (in Russian)
- [10] S.E. Aleksandrov, G.A. Gavrilov, A.A. Kapralov, B.A. Matveev, G.Yu. Sotnikova, M.A. Remenny. *ZhTF*, **79**(6), 112 (2009) (in Russian).
- [11] A.V. Zagnitko, A.A. Kirsh, I.B. Stechkina. *ZhFKh*, **62** (11), 3058 (1988) (in Russian).
- [12] J. Broeke, J.M. Perez, J. Pascau. *Image Processing with ImageJ. 2-nd edition* (London, Packet Publishing, 2015), 256 p. ISBN 978-1-78588-983-7.
- [13] A.N. Ishmatov. *Polzunovskij vestnik*, (3), 175 (2010) (in Russian).
- [14] V.K. Kedrinsky. *Gazodinamika vzryva: eksperiment i modeli* (Novosibirsk, SO RAN, 2000), 435 s. (in Russian)
- [15] S.V. Stebnovsky. *Fizika goreniya i vzryva*, **44** (2), 117 (2008). (in Russian)